UK Heat Transfer Conference 2021
UKHTC2021

17th UK Heat Transfer Conference (UKHTC2021)
4-6 April 2022, Manchester, UK

# DETAILED EXPERIMENTAL CHARACTERISATION OF FLOW BOILING IN HORIZONTAL PIPES USING LASER-DIAGNOSTIC TECHNIQUES

**Hannah R. Moran[1], Victor Voulgaropoulos[1], Shunsuke Yamada[2], Omar K. Matar[1], Christos N. Markides[1,3,*]**

[1] Department of Chemical Engineering, Imperial College London, London SW7 2AZ, United Kingdom
[2] Department of Mechanical Engineering, Det, Yokosuka, Kanagawa, Japan
[3] Kutateladze Institute of Thermophysics, Novosibirsk, Russian Federation

## ABSTRACT

Flow boiling in horizontal pipes occurs in a wide range of applications, including in direct steam generation concentrating solar power plants. Subject to the heat and mass flux conditions and the local vapour quality, many different flow patterns can develop, creating a complex transient two phase flow. The detailed characterisation of the these flows will aid understanding of the underlying phenomena and therefore improve the design and operation of flow boiling systems. As such, a bespoke experimental facility is employed to collect investigate boiling R245fa flows in a 12.6 mm diameter horizontal stainless steel pipe. Flow patterns are identified through high-speed imaging, with the results being compared to existing flow pattern maps in the literature. Integral measurements are complemented in this work by detailed spatiotemporally resolved information on interface location and liquid-phase velocity fields obtained through the application of advanced laser diagnostic techniques such as particle image velocimetry (PIV) and planar laser induced fluorescence (PLIF). Methods such as these have been used extensively in multiphase flows without phase change, and in pool boiling, but have rarely been employed to study boiling flows. This work therefore provides new insights into the thermohydraulic behaviour of boiling flows, and provides a basis for further develop of laser diagnostic methods under these conditions.

## 1. INTRODUCTION

Numerous applications of boiling flows in horizontal pipes exist, including power generation with steam or organic Rankine cycle (ORC) systems [1], e.g., in concentrating solar power plants [2], as well as heat pumps, refrigeration systems, and many others. The inherently complex nature of these transient two-phase flows presents a challenge for technology innovation and development, system design and optimisation, reliable control and operation, thus creating the need for fundamental understanding of the hydrodynamic and heat transfer characteristics of horizontal flow boiling.

Integral quantities such as pressure gradients and heat transfer coefficients have been measured for flow boiling of a wide range of fluids across different pipe sizes [3,4], and various flow conditions; pattern maps have been proposed to characterise the different interfacial structures, such as that of Wojtan et al. [5]. However, there is a scarcity of detailed spatiotemporally resolved data/information generated during boiling flows in horizontal pipes, such as interfacial dynamics, phase distributions and velocity fields, amongst other. Laser-diagnostic techniques based on particle image velocimetry (PIV) and laser-induced fluorescence (LIF) have previously been applied to two-phase flows to provide such data [6-8], and most recently to pool boiling systems [9]. Such measurements could reveal insights into the thermohydraulic behaviour of boiling flows, and provide validation cases for numerical simulations.

## 2. METHODOLOGY

A bespoke experimental facility at Imperial College London, whose overall layout is illustrated in Fig. 1a, has been constructed and has been employed in the present work to investigate flow boiling of R245fa in horizontal pipes using laser-based measurement techniques.

---

*Corresponding Author: c.markides@imperial.ac.uk

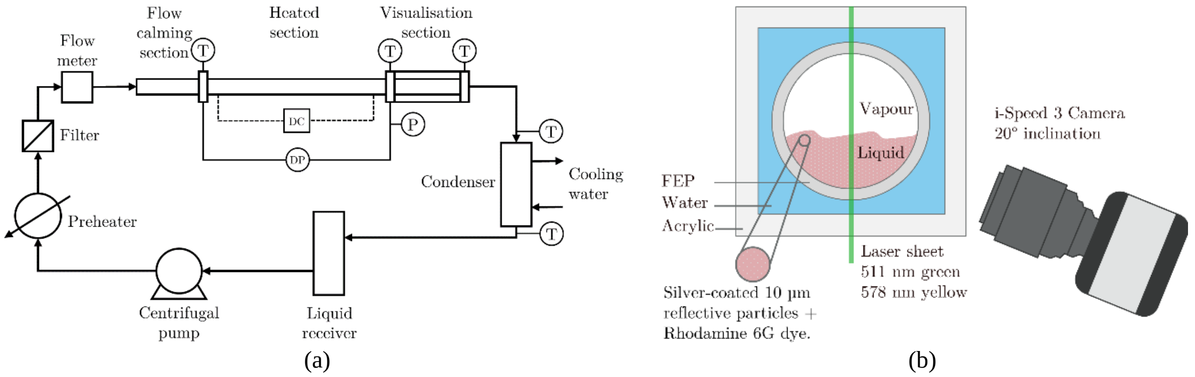

(a) (b)

**Figure 1**: (a) Flow diagram of the flow boiling facility at Imperial College London. Measurement locations for temperature, pressure and differential pressure are indicated in the figure by symbols 'T', 'P' and 'DP' respectively. (b) Experimental arrangement for combined PIV and PLIF measurements in horizontal two-phase stratified flows.

The flow circuit consists of a vertical liquid receiver, pump, preheater, heated test section, visualisation section, condenser, and various instrumentation for measurement and control. The test section is a 2 m long, 12.6 mm inside-diameter stainless steel pipe, preceded by a 0.6 m long flow straightening section of the same geometry and material. The test section is heated by direct current application from a 20 V, 750 A power supply providing uniform heat flux of up to 135 kW/m$^2$.

During experiments, the in-flow fluid temperature is measured at the inlet and outlet of the heated test section and visualisation section, whilst wall temperature measurements are taken at junctions along the heated section. The heat transfer coefficient can be calculated based on these measurements. Pressure drops are measured across the heated test section, whilst the absolute pressure is measured at its outlet.

The visualisation section is designed to allow the application of laser-based diagnostic techniques, specifically planar laser-induced fluorescence (PLIF) and particle image velocimetry (PIV). The flow is illuminated by a laser sheet generated by a copper-vapour laser that emits two narrow band laser beams at 510.6 nm (green light) and 578.2 nm (yellow light) at a nominal output power of 20 W, frequency of 2 kHz, pulse-duration of 2 ns, and pulse energy of 2 mJ. The beams are directed to a sheet generator via a fibre-optic cable, with the sheet expanded in the streamwise direction and illuminating the flow in a plane through the (axial) centreline of the pipe from the bottom of the correction box.

An i-Speed 3 high-speed camera, mounted at an angle of approximately 20° from the horizontal and fitted with a corrective Scheimpflug filter, is used to capture instantaneous images of the illuminated flow. In the present work, images were captured at a frame rate of 1500-2000 fps, depending on the flow. A series of post-processing steps are applied to the high-speed images captured in this arrangement in order to extract the interface location (from PLIF) and velocity fields (from PIV). These data are analysed to provide interface and wave statistics, and detailed spatiotemporally resolved information on the liquid phase velocity. A full description of the image processing steps is given in Moran [10].

## 3. RESULTS

Experimental data were collected in the flow boiling facility described in the previous section for conditions with heat and mass fluxes in the ranges $q = 0.5 – 38$ kW/m$^2$ and $G = 30 – 700$ kg/m$^2$.s, and at a saturation pressure of 1.7 bar. Flow patterns were identified using high-speed imaging and are compared to the predictions made by the flow pattern map of Wojtan et al. [5] in Fig. 2. This method accurately predicted 80 % of flow patterns, with the majority of deviations in the stratified, stratified-wavy and slug + stratified-wavy regimes. Heat transfer coefficient and pressure drop data were also obtained for each of the experimental data points in Fig. 3, and can be used to validate predictive methods in the literature for the flow conditions investigated in this work.

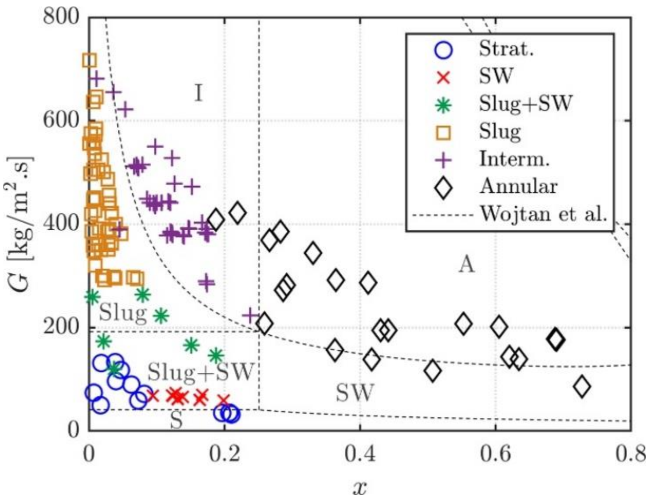

**Figure 2**: Flow pattern map summarising all experimental data points at a saturation pressure of 1.7 bar. Transition lines have been calculated according to the method of Wojtan et al. [5] for a heat flux of 14 kW/m$^2$ and a mass flux of 332 kg/m$^2$.s.

Detailed spatiotemporally resolved information on phase distributions and liquid-phase velocity fields have been obtained in selected stratified and stratified-wavy flows using a combined PLIF and PIV technique. Figure 3 shows time-averaged liquid-phase velocity profiles in the streamwise direction for stratified flows over a range of mass fluxes from $G = 32$ to 131 kg/m$^2$.s. At low mass fluxes, the velocity increases steadily away from the wall and reaches a maximum close to the interface, as expected for laminar stratified flows. As the mass flux increases, the corresponding Reynolds number increases and the flows become first transitional and then turbulent; as such, the velocity profiles flatten with a larger maximum velocity reached further from the liquid-vapour interface.

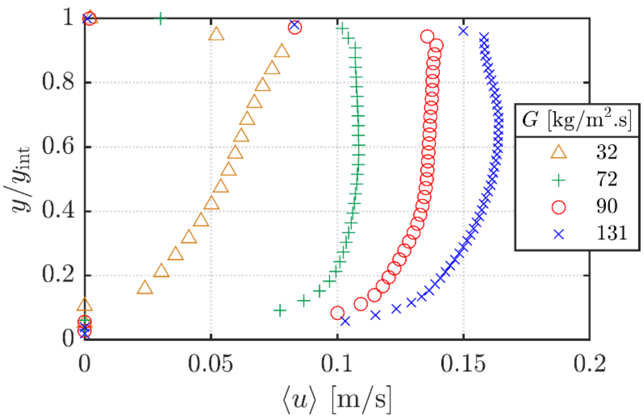

**Figure 3**: Time-averaged liquid-phase streamwise velocity profiles for stratified flows with $q = 1.7$ kW/m$^2$ and for a range of mass fluxes, with the vertical coordinate $y$ scaled by the interface height $y_{\text{int}}$.

Figure 4 shows instantaneous velocity fields in stratified-wavy flows at two conditions. In both plots, the streamwise velocity increases from the bulk underneath the wave peak, with the highest velocity on the back slope of the wave. Figure 4b reveals higher velocities both in the bulk and in the wave crest than Fig. 4a despite the mass flux $G$ being similar. This is because the flow in Fig. 4b is subject to a higher heat flux $q$, resulting in the evaporation of more of the liquid phase and, therefore, a higher vapour quality $x$ and void fraction. This can be seen in the relative interface heights of the flows in the two plots, with that in Fig. 4b being lower. The wave height relative to that between the waves is also higher in the flow in Fig. 4b, indicating enhanced waviness due to the higher heat flux. The liquid phase Reynolds numbers of the flows in Figs. 4a and 4b, respectively, are 9430 and 11 000, corresponding to the higher velocities and increased turbulence levels in the latter.

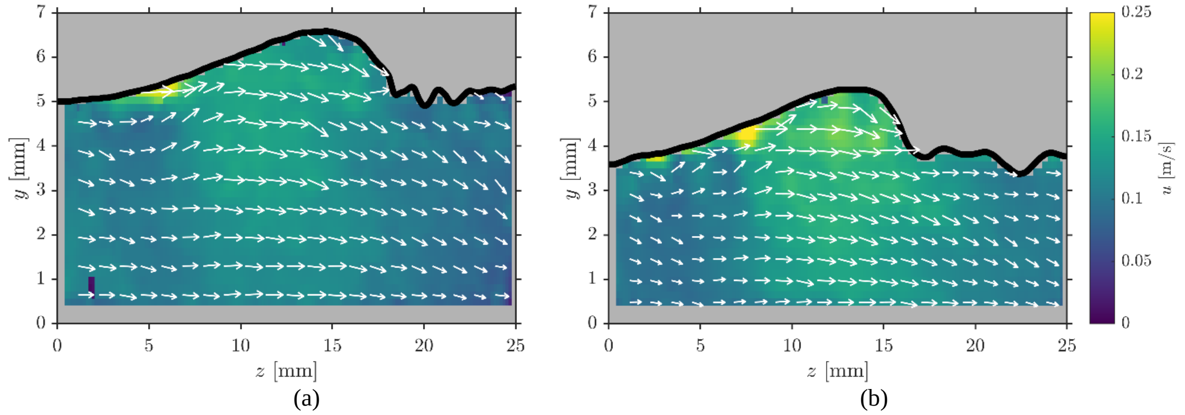

(a)

(b)

**Figure 4**: (a) Instantaneous velocity fields in a stationary frame of reference in stratified-wavy flows with: (a) $G = 73$ kg/m$^2$.s, $q = 2.6$ kW/m$^2$, and (b) $G = 70$ kg/m$^2$.s, $q = 3.4$ kW/m$^2$. The vapour-liquid interface is marked with a black line, and has an uncertainty of ± 0.16 mm.

It can be seen from the changes in direction of the arrows in Fig. 4 that the wave induces secondary flows, particularly at the crest of the waves where the flow accelerates in both the streamwise and vertical directions. These secondary flows, particularly as waves become larger, can move liquid away from the heated wall as they disturb the layer of unidirectional streamwise flow close to the wall. The presence of non-zero vertical components of velocity is demonstrated in both flows in Fig. 4, with the flow close to the interface accelerating upwards in the back of the wave (i.e., the left-hand side) then downwards out of the wave front. This downward motion is carried into the bulk ahead of wave, with the vertical component of the velocity decreasing in magnitude towards the wall. As a result, hot fluid close to the heated tube wall is displaced and replaced with cooler fluid, which increases the temperature gradient between the wall and the liquid and, consequently also, increases the heat transfer rate locally. For the stratified-wavy flow shown in Fig. 4a the average heat transfer coefficient is 26 % larger than that for a stratified flow of equal heat flux and 45 % larger mass flux.

Since the heat transfer coefficient generally decreases with decreasing mass flux in convective boiling [11, 12], this increase for the stratified-wavy flow is likely to be a result of the flow structures described above. This effect was found to be consistent across all investigated conditions with comparable heat flux, suggesting a pronounced heat transfer enhancement due to interfacial waviness.

For multiple stratified-wavy flow conditions, the mean interface height, was calculated by averaging the interface height across all pixels and frames for, whilst an interfacial roughness was calculated as the ratio of the root mean square of the interface heights across all pixels and frames for each case, normalised by the corresponding mean interface height. The dimensionless heat transfer, expressed in terms of the Stanton number, $St = h/Gc_{\mathrm{p,l}}$, is plotted as a function of these two variables for both stratified and stratified-wavy flows in Fig. 5.

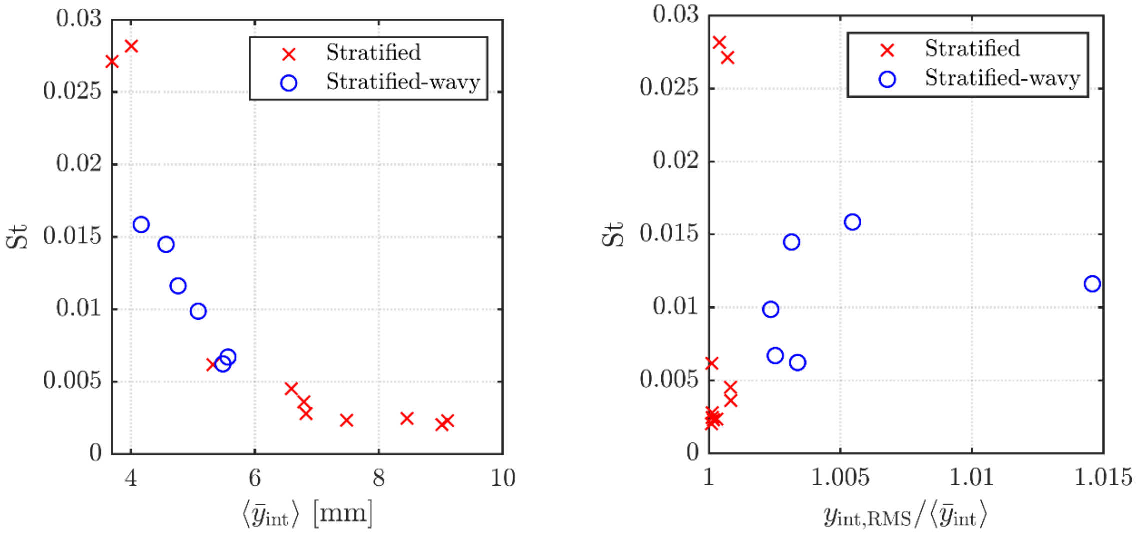

(a) (b)

**Figure 5**: Stanton number ($St = h/Gc_{\mathrm{p,l}}$) as a function of: (a) mean interface height, and (b) interfacial roughness for stratified and stratified-wavy flows.

Figure 5a shows that, in general, the mean film thickness was greater in the stratified flows than the stratified-wavy flows investigated in the present campaign. To achieve stratified flows as opposed to stratified-wavy flows, lower heat flux conditions were mostly used, resulting in reduced evaporation of the liquid phase and a higher liquid-vapour interface. The two points at approximately 4mm correspond to a stratified flow condition with low mass flux and relatively high heat flux. Figure 5b shows that interfacial roughness was higher for stratified-wavy flows than stratified flows. However, the magnitude of the interfacial roughness for stratified-wavy flows indicates that they are not dominated by large disturbance waves, in which case the roughness would be expected to be much higher.

From Fig. 5a, it can be deduced that that heat transfer decreases with increasing interface height in the lower half of the pipe (note that $d = 12.6$ mm), particularly for stratified-wavy flows. Thin film heat transfer enhancement has been observed in heated falling films [13], where a thinner film presents lower resistance to heat transfer and will be proportionally more affected by interfacial waves and disturbances resulting in more efficient replacement of warm fluid at the wall with colder fluid.

Aside from the two points in the top left, Fig. 5b suggests that increasing interfacial roughness enhances heat transfer, although the correlation is not definitive enough to completely isolate this effect. However, this behaviour is in line with observations of heat transfer enhancement due to film waviness reported for film flows [13] caused by increased mixing. The two outlier points correspond to cases with very low mass fluxes, higher heat fluxes and consequently very thin films, suggesting that the thin film heat transfer enhancement is dominant over the enhancement due to film waviness for these conditions.

## 4. CONCLUSIONS

A flow boiling facility with a suitable optical test section where optical, laser-based measurements can be performed has been designed, commissioned and employed to obtain both integral and detailed spatiotemporally resolved measurement data of the flow boiling of R245fa in a horizontal pipe of inside diameter 12.6 mm over a range of conditions. The integral thermohydraulic data were compared to predictive methods in the literature, whilst the application of laser-based techniques provided insights into the velocity fields in stratified and stratified-wavy flows.

Laser-induced fluorescence was employed to identify the vapour-liquid interface in stratified flows, whilst particle image velocimetry was used to investigate the liquid phase velocity fields. The streamwise velocity profiles for laminar inlet conditions conformed to theoretical predictions, whilst the heat transfer coefficient was found to increase with decreasing interface height due to conduction through the thin film. The presence of interfacial waves was found to enhance heat transfer in stratified-wavy flows compared to stratified flows, but the stratified-wavy flows investigated did not exhibit large disturbance waves or the corresponding recirculation flows in the liquid phase.

The detailed spatiotemporally resolved measurements presented here represent an important contribution to the literature and can provide insights into the interaction of hydrodynamic and heat transfer phenomena in boiling flows. This could improve the design and operation of boiling systems including refrigeration and heat-pump systems, waste-heat recovery and conversion systems and concentrating solar power technology. The data can also be used for advanced multiphase model development and validation, and the techniques presented here can be used to investigate additional flow patterns common to flow boiling applications such as slug flow and annular flow.

## ACKNOWLEDGEMENTS

This work was supported by Russian Government “Megagrant” project 075-15-2019-1888, the UK Department for International Development (DFID) through the Royal Society-DFID Africa Capacity Building Initiative, and the UK Engineering and Physical Sciences Research Council (EPSRC) [grant numbers EP/P004709/1 and EP/L020564/1]. Data supporting this publication can be obtained on request from cep-lab@imperial.ac.uk.

## REFERENCES

[1] C.N. Markides, Low-concentration solar-power systems based on organic Rankine cycles for distributed-scale applications: Overview and further developments. *Front. Energy Res*, **3** (2015), 47:1-16.

[2] J. Dirker, et al.,Thermal energy processes in direct steam generation solar systems: Boiling, condensation and energy storage–A review. *Front. Energy Res.*, **6** (2019), 147:1-35.

[3] O. Turgut, M. Coban & M. Asker, Comparison of Flow Boiling Pressure Drop Correlation for Smooth Macrotubes. *Heat Transfer Eng.,* **37** (2016), 487-506.

[4] X. Fang, F. Zhuang, C. Chen, Q. Wu, Y. Chen, Y. Chen & Y. He, Saturated flow boiling heat transfer: review and assessment of prediction methods. *Heat Mass Transf.*, **55** (2018), 197-222.

[5] L. Wojtan, T. Ursenbacher, & J.R. Thome, Investigation of flow boiling in horizontal tubes: Part I – A new diabatic two-phase flow pattern map. *Int. J. Heat Mass Transf.*, **48** (2005), 2955–2969.

[6] A.V. Cherdantsev, J.S. An, A. Charogiannis, & C.N. Markides, Simultaneous application of two laser-induced fluorescence approaches for film thickness measurements in annular gas-liquid flows. *Int. J. Multiph. Flow,* **119** (2019), 237-258.

[7] I. Zadrazil, O.K. Matar, & C.N. Markides, An experimental characterisation of downwards annular flow by laser-induced fluorescence: Flow regimes and film statistics. *Int. J. Multiph. Flow,* 67 (2014), 42-53.

[8] A. Charogiannis & C.N. Markides, Spatiotemporally resolved heat transfer measurements in falling liquid-films by simultaneous application of planar laser-induced fluorescence (PLIF), particle tracking velocimetry (PTV) and infrared (IR) thermography. *Exp. Therm. Fluid Sci.,* **107** (2019), 169-191.

[9] V. Voulgaropoulos, G.M. Aguiar, C.N. Markides, & M Bucci, Simultaneous laser-induced fluorescence, particle image velocimetry and infrared thermography for the investigation of the flow and heat transfer characteristics of nucleating vapour bubbles. *Int. J. Heat Mass Transf.*, **187** (2022), 122525.

[10] H.R. Moran, *Flow boiling in horizontal pipes: integral measurements, optical diagnostics, and numerical simulations* (2021), Imperial College London.

[11] B.K. Hardik & S.V Prabhu, Boiling pressure drop and local heat transfer distribution of water in horizontal straight tubes at low pressure. *Int. J. Therm. Sci.*, **110** (2016), 65-82.

[12] Q. Guo, M. Li & X. Tian, Experimental study on flow boiling heat transfer characteristics of R134a, R245fa and R134a/R245fa mixture at high saturation temperatures, *Int. J. Therm. Sci.*, **150** (2020), 106195.

[13] R. Mathie, H. Nakamura & C.N. Markides, Heat transfer augmentation in unsteady conjugate thermal systems - Part II: Applications *Int. J. Heat Mass Transf.,* **56** (2013), 819-833.